Journal of Research and Applications in Mechanical Engineering
ISSN: 2229-2152 (Print); 2697-424x (Online)
(2025) Vol. 13, No. 2, Paper No. JRAME 25-13-028
[DOI: 10.14456/jrame.2025.28]

Research Article

Influence of Delta Winglets on Improving heat transfer and friction factor characteristics in tubular heat exchanger

K. Ruengpayungsak[1]
P. Samruaisin[1]
P. Kaewkosum[2]
S. Pingta[3]
K. Wongcharee[3]
A. Phila[1]
S. Eiamsa-ard[1]
P. Thapmanee[3,*]
[1] Department of Mechanical Engineering, School of Engineering and Industrial Technology, Mahanakorn University of Technology, Bangkok, 10530 Thailand
[2] School of Engineering, King Mongkut's Institute of Technology Ladkrabang, Bangkok, 10520 Thailand
[3] Department of Process and Industrial Engineering, School of Engineering and Industrial Technology, Mahanakorn University of Technology, Bangkok, 10530 Thailand

Received 9 October 2024
Revised 26 November 2024
Accepted 26 November 2024

Abstract:
Heat transfer rate and pressure drop characteristics are two critical constraints that substantially influence the advancement of solar air heaters. The thermal efficacy of these systems is significantly improved by factors such as flow configurations, thermal mechanisms, and geometric modifications. The integration of insertion in turbulators is a common method to improve heat transfer efficiency in solar air heaters. This article presents heat transfer and thermal efficiency in a tubular heat exchanger incorporating Delta winglet (DW). The thermal transfer and pressure drop of air as a working fluid in a tube with a constant heat flux were quantified for Reynolds numbers (Re) between 6000 and 20,000. The DW elements were positioned on two tape sides in a configuration with attack angles (θ) of 30°, 45°, and 60°. Delta winglet height ratios (h/D=0.10) and pitch ratios (p/D=0.1) were examined. Data from the current smooth or plain tubes were also analyzed for comparative purposes. According to the experimental results, the tube with this inserted has a much higher Nusselt number (Nu) and friction factor (f) than a plain tube. Both Nu and f increase as θ decrease. The DW enhances Nu and f by approximately 2.51-3.04 times and 5.21-7.16 times, respectively. The maximum TEF of 1.34 is achieved at an attack angle of 30° and a Reynolds number of 6000. The statistical correlations for Nu f and TEF were analysed and demonstrated a strong fit to the observed data, with discrepancies of ±4%, ±5% and ±3%, respectively. This design improves the conservation of energy in heat exchanger tube applications.

Keywords: *Heat transfer enhancement, Delta winglet, Nusselt number, thermal enhancement factor*

1. Introduction

Heat exchangers play a vital role in numerous engineering applications, including vortex combustors, internal cooling of gas turbine blades, thermal regenerators, electronic cooling systems, and solar water heaters. Traditional heat exchangers with plain tubes often exhibit poor performance due to low heat transfer coefficients and inefficient thermo-hydraulic characteristics. This inefficiency results in increased energy consumption and diminished economic returns. The rising demand for high-performance thermal systems has led to the development of advanced heat transfer enhancement techniques designed to improve heat transfer rates, reduce the size of heat exchangers, and boost overall system efficiency. These techniques include various methods to roughen surfaces or insert devices, such as ribs [1–3], coiled wires [4–6], baffles [7,8], winglet vortex generators [9–12], rings [13,14], vortex rod/conical strip vortex generators [15–17], V-shaped rings [18], and twisted tapes [19–21].

These techniques promote the mixing of core fluid with near-wall fluid, enhancing convective heat transfer.

* Corresponding author: P. Thapmanee
E-mail address: piphatpong@mut.ac.th

Among the commonly employed strategies to augment heat transfer in single-phase internal flows, the installation of ribs, baffles, and winglets along the walls of cooling or heating channels has gained prominence. These devices not only disrupt the boundary layer development but also induce stronger turbulence, improving fluid mixing and heat transfer. Promvonge and Skullong [22] conducted an experimental study on the effects of a straight tape with double-sided V-baffles as a longitudinal vortex generator on turbulent convection heat transfer behaviors in a heat-fluxed tube. The study tested V-down and up tapes with different baffle heights and pitch ratios. The results showed that the V-down tape generally yielded higher heat transfer, friction loss, and thermal performance than the V-up tape. Under optimal conditions, with a blockage ratio (*RB*) of 0.15 and a pitch ratio (*RP*) of 1.0, a maximum thermal performance enhancement factor (*TEF*) of 2.07 was achieved. A 3D numerical V-baffled-tube flow model was simulated to examine fluid flow and heat transfer patterns. The numerical validation was found to be in close agreement with the experimental data. Sumannapan et al. [23] employed zigzag-winglet perforated-tape inserts (ZW-PT) within a cylindrical tube for turbulent airflow, for $4{,}200 \leq Re \leq 26{,}000$. The ZW-PT was introduced into the test tube at varying pitch and blockage ratios. The findings indicated that the Nusselt number and friction factor rose with increasing *BR* and *Re*, but they diminished with decreasing *PR*. The Nusselt number for the tube with inserts was 3.1 to 5.1 times greater than that of the plain tube, while the friction factor was approximately 12.5 to 53.6 times higher. Employing ZW-PT with *PR*=1.0 resulted in an improved thermal enhancement factor (*TEF*) of 3-5%. Three-dimensional numerical simulations were also performed to assess the turbulent flow, temperature distribution, and local Nusselt number field in a circular tube heat exchanger equipped with sinusoidal baffles, positioned at the center of the tube to act as turbulators. The simulations, conducted at Reynolds numbers between 5,000 and 20,000, revealed that the sinusoidal baffles deflected fluid flow and improved heat transfer along the tube walls. The results demonstrated that the sinusoidal baffles provided higher Nusselt numbers and friction factors than plain tubes. Overall, the heat transfer, friction factor, and *TEF* were 1.7–7.7, 3.6–117 and 1.12–1.9 times higher, respectively, than those of plain tubes. The maximum TEF of 1.9 was observed at a *PR* of 2.0 and an aspect ratio (*AR*) of 0.20, at a Reynolds number of 5,000. Promthaitsong and Sumannapan [24] and Prasopsuk et al. [25] examined thermal characteristics in a constant heat-fluxed circular tube with rectangular-winglet tape (RWT) vortex generators. The working fluid was air, with Reynolds numbers between 4,100 and 26,000. The impact of the RWT insert on the heat transfer rate and friction loss was investigated. The results showed that heat transfer and friction loss increased with the increment of *BR*. The inserted tube had a higher *Nu* (3.7-4.3 times higher) and *f* (19.4-45 times greater). The highest thermal enhancement factor (η) was obtained for *BR*= 0.2 at the lowest *Re*. Promthaisong and Skullong [26] investigated the effects of diamond-shaped rings (DRs) installed in a heat-fluxed heat exchanger tube on flow resistance and thermal behavior. The DR elements, designed to generate longitudinal vortex flows, were connected by two small rods. The study examined the influence of three different relative ring pitches and three ring blockage ratios on the Nusselt number (*Nu*), friction factor (*f*), and thermal enhancement factor (*TEF*) within turbulence regimes, with Reynolds numbers (*Re*) ranging from 4,000 to 26,000. The results revealed that both heat transfer and pressure loss increased with higher *RB* values but decreased as *RP* values lowered. The maximum *Nu* and *f* were achieved at an *RB* of 0.2 and an *RP* of 0.5, while the highest *TEF* was recorded at an *RB* of 0.10 and an RP of 1.0. Empirical correlations for *Nu, f* and *TEF* were developed, showing a good fit with the experimental data.

Thianpong et al. [27] reported the thermal performance, pressure loss, and heat transfer characteristics of a round conduit equipped with twisted rings. The experiments utilized twisted rings with three different pitch ratios (*p/D*) and three width ratios (*W/D*). The results indicated that twisted rings exhibited lower heat transfer rates and friction factors compared to conventional circular rings. Moreover, the heat transfer rate and friction factor increased with a larger width ratio and a smaller *p/D*. The highest thermal performance factor was associated with twisted rings having the smallest *W/D* and *p/D*. Singh et al. [28] examined the heat transfer and fluid flow characteristics of a tube with roughened surfaces under continuous heat flux. Solid ring inserts with two different pitch ratios and twisted tape inserts with three distinct twist ratios were employed. Vortex flow was generated within the test section of the tube using inserts. The study found that the highest thermal performance was achieved when four co-twisted tape inserts were arranged. Promvonge and Skullong [29] studied turbulent convective heat transfer in a constant heat-fluxed tube, focusing on the effects of inserting a straight tape with double-sided V-baffles, which acted as a longitudinal vortex generator (LVG). In their experiment, the V-shaped baffles were placed on the tape at a fixed attack angle (α = 30°) in two configurations: "V-down" (V-apex pointing upstream) and "V-up" (V-apex pointing downstream). The baffles were tested with three different baffle height ratios (0.1 to 0.2) and pitch ratios (0.5 to 1.5). The results demonstrated that the V-down tapes outperformed the V-up tapes in enhancing both heat transfer and thermal performance factors. Rahman and Dhiman [30] investigated the use of a novel flow deflector-type baffle plate in a turbulent circular heat exchanger. The study focused on evaluating the performance of this heat exchanger, particularly in terms of heat transfer and flow characteristics. The circular baffles equipped with flow deflectors introduced swirl flow, increasing turbulence and enhancing the heat transfer rate. The deflector design optimized the swirling effect, which contributed to superior thermal performance compared to traditional baffle configurations. The results demonstrated that the deflector-type baffle plates significantly enhanced the heat transfer efficiency while maintaining manageable pressure losses. Jayranaiwachira et al. [31] studied the effect of louvered curved baffles on the thermohydraulic performance of heat exchanger tubes. The study explored how variations in baffle configurations impacted both heat transfer and pressure drop, highlighting the trade-off between these two factors. The results revealed that the louvered curved baffles improved the heat transfer significantly, particularly at higher Reynolds numbers, where turbulence levels were elevated. However, the pressure drop increased correspondingly, which must be considered in practical applications where pumping power is a concern. Wang et al. [32] introduced a novel approach to heat transfer enhancement in copper tubes using perforated teardrop-shaped turbulators (PTST). This study aimed to improve heat transfer in tubes with constant wall temperatures by employing turbulators with a unique teardrop shape, designed to induce swirling motions in the flow. The perforations further contributed to breaking up the flow patterns, reducing boundary layer thickness and enhancing overall heat transfer. The research found that the teardrop turbulators not only improved heat transfer rates but also reduced the temperature gradients along the tube walls. Kumar et al. [33] conducted an experimental analysis of heat exchangers equipped with perforated conical rings, twisted tape inserts, and CuO/H_2O nanofluids. This study combined passive techniques with advanced working fluids (nanofluids). The nanofluids, with their enhanced thermal conductivity, played a key role in increasing the heat transfer capacity, while the twisted tape inserts generated swirling flows that further improved the thermal performance.

Recent studies highlight the impact of vortex generators (VGs) on enhancing heat transfer in various heat exchanger configurations. Ejaz et al. [34] achieved enhanced flow and blockage rates by placing a single vortex generator at the duct entrance, which improved flow and temperature distribution through increased recirculation. Song et al. [35] introduced an optimized wavy delta winglet vortex generator (VG) for fin-and-tube heat exchangers, showing that the VG's attack angle, central angle, and arrangement significantly impact heat transfer and friction. Their results indicated that the VG design enhanced secondary flow intensity and thermal performance by up to 1.29 times, providing theoretical insights for fin-and-tube heat exchanger optimization. Yuan et al. [36] developed a model to enhance heat transfer in spiral finned tubes (SFTs) using triangular winglets, verified through particle image velocimetry. The findings revealed that SFTs with triangular winglets outperform conventional SFTs, with the heat transfer coefficient increasing as the number of winglets rises. Meanwhile, Heriyani et al. [37] improved heat transfer in rectangular ducts by installing perforated concave rectangular winglet pair VGs (PCRWP VGs) on plates. Their study found that the in-line VG configuration achieved a superior cost-benefit ratio (3.56) and thermal performance over the staggered configuration, resulting in a more efficient heat transfer system. Together, these studies confirm the versatility of VG designs in boosting heat exchanger efficiency with manageable energy costs.

According to the literature review, winglet turbulators are widely utilized for their advanced design features. These turbulators are specifically designed to generate longitudinal vortices-spiraling fluid motions that run parallel to the main flow direction. Unlike other common turbulators, delta winglets introduce a more streamlined design, which minimizes pressure drop and, consequently, reduces the energy required to maintain fluid flow through the system. In general, winglet-mounted configurations are employed in rectangular ducts and fin-tube heat exchangers, due to their ease of integration onto flat surfaces. However, their application in tubular heat exchangers has been limited, primarily due to the difficulties in mounting winglets on curved surfaces. A practical solution to this challenge involves attaching the winglets to a straight flat tape, which can then be inserted into the tube, enabling convenient incorporation into tubular systems.

Considering the challenges and recent advancements in heat transfer enhancement, this study aims to improve the performance of heat exchange pipes by inserting Delta winglets. The investigation focuses on the effects of key parameters, including baffle height ratio (h/D = 0.10), pitch ratio (p/D = 0.1), and attack angles (θ = 30°, 45° and 60°). The selection of these specific parameters is guided by reference literature, which highlights their significance in optimizing heat transfer performance. Studies indicate that these parameters play a critical role in enhancing turbulence intensity and disrupting boundary layer development, both of which are essential for improving convective heat transfer within the channel. Specifically, the chosen attack angles offer varied levels of flow deflection, while the selected height and pitch ratios have been shown to effectively balance heat transfer gains with manageable friction losses, using air as the working fluid in a turbulent flow regime with Reynolds numbers (Re) ranging from 6,000 to 20,000. Additionally, the study compares the performance of Delta winglets with that of plain tubes and provides empirical correlations for Nusselt number, friction factor and thermal enhancement factor (TEF).

2. Experimental Setup

2.1. Configuration of Delta winglet (DW)

The configurations of the Delta winglet (DW) elements and the test tube containing the device are depicted in Fig. 1 and 2. A copper tube with an inner diameter of 38 mm, a thickness of 4 mm, and a test section length of 1200 mm was used as the test tube. The Delta winglets were mounted at regular intervals on both sides of a straight tape, forming a series of winglets along the tape, as shown in Fig. 1. The plate had a length of 1200 mm, a thickness of 0.8 mm, and a winglet thickness of 4 mm. A pitch ratio of 0.10 and a height ratio of h/D = 0.10 were employed. The tapes were configured with Delta winglets at attack angles of θ = 30°, 45° and 60° relative to the axial direction and were positioned at the center of the tube along the core flow, as illustrated in Fig. 2. The detailed parameters and test conditions are provided in Table 1.

2.2. Overview of procedures and experimental techniques

The experimental setup for heat transfer analysis, as illustrated in Fig. 3, incorporates a test tube designed in line with TEMA standards to ensure optimal flow distribution, reduced pressure drop, and a balance between heat transfer efficiency and fluid resistance within the test section. In this configuration, air at 25±0.5°C, powered by a 1.5 kW input, is directed through an orifice flow meter. The airflow rate, calibrated with a hot-wire anemometer, is regulated by adjusting compressor speed via an inverter. To maintain a uniform heat-flux boundary, flexible electrical heating wires wrap the insulated test tube. Temperature readings are taken with a multi-channel system using RTD PT-100 sensors (accuracy ±0.1°C) at inlet and outlet points, while 10 T-type thermocouples positioned along the top and side walls monitor surface temperatures (T_w). The pressure drops across the test section, measured using a digital manometer with ±1% accuracy, provide essential data for evaluating flow characteristics. Reynolds numbers from 6,000 to 20,000 are achieved by varying blower speed, enabling a comprehensive analysis of heat transfer performance across different flow conditions. Overall, the uncertainties reported above are well within the acceptable ranges commonly observed in industry practices.

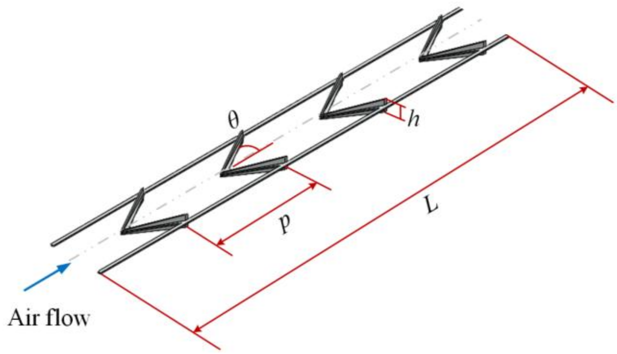

(a)

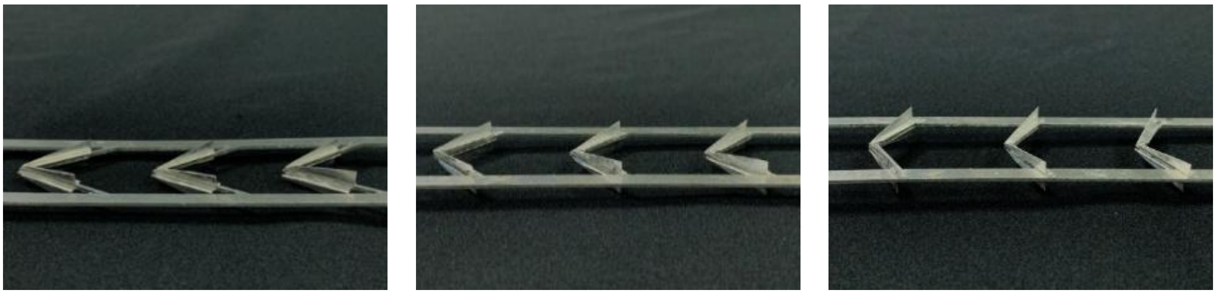

θ = 30 ° θ = 45 ° θ = 60 °

(b)

Fig. 1. (a) Configuration of Delta winglet (DW) and (b) Attack angle

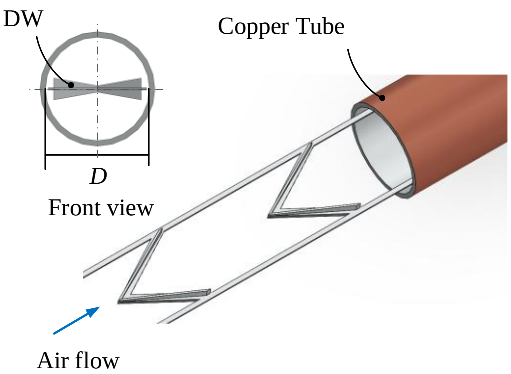

Fig. 2. Test section with DW inserts

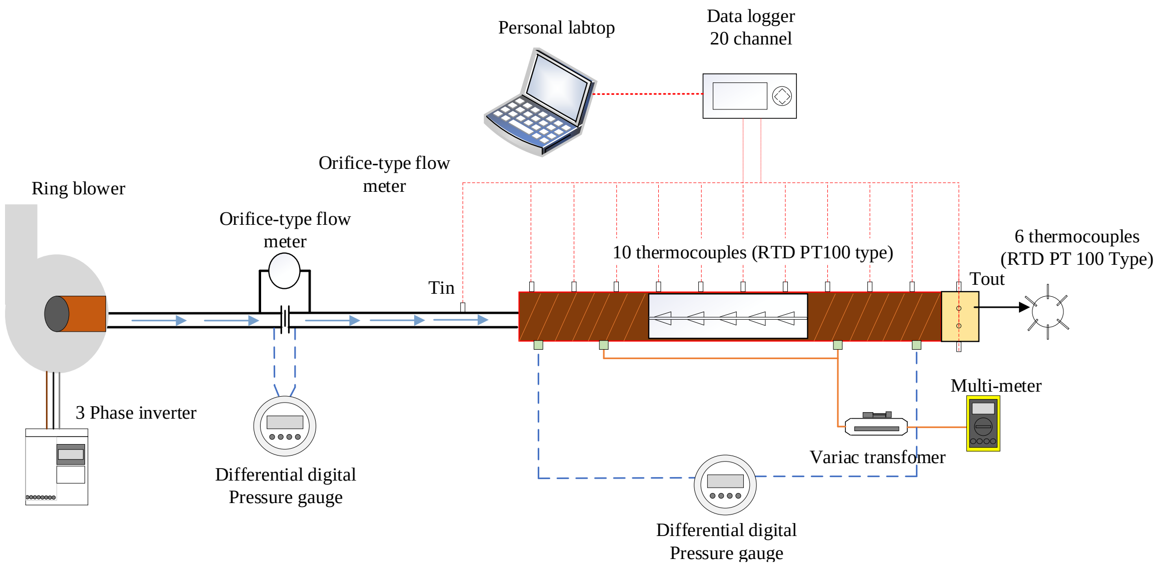

Fig. 3. Schematic diagram of the experimental setup

Table 1: Ranges of parameters in the investigation

Experimental parameters	Details and ranges of condition		
Flow attack angle (θ)	30°	45°	60°
The pitch ratio (*p/D)*		0.10	
DW height ratios (*h/D)*		0.10	
DW thickness (*e*)		4.0 mm	
Test tube diameter (*D*)		38 mm	
Test tube length (*L*)		1,200	
Plate thickness (*t*)		0.8 mm	
Reynolds number (*Re*)		6,000-20,000	
Working fluid		Air	
The inlet temperature of air (T_i)		25°C	

3. Data Processing

This section describes the data reduction for the following variables: pressure drop (friction factor, *f*), thermal enhancement factor (at the same pumping power, TEF), heat transfer rate (Nusselt number, *Nu*), and flow condition (Reynolds number, *Re*). Given the tube diameter, the Reynolds number (*Re*) is calculated by the following formula

$$\mathrm{Re} = UD/\nu \tag{1}$$

The pressure loss across the test tube length to determine the f is expressed as

$$f = \frac{\Delta P}{\left(\frac{L}{D}\right)\left(\rho\frac{U^2}{2}\right)} \tag{2}$$

where U is the test tube's mean air velocity.
In the experiment, air flowed through the test tube under a constant heat flux. The rate of heat convection is assumed to be equivalent to the steady-state heat transfer rate of the air.

$$Q_a = Q_{\mathrm{conv}} \tag{3}$$

where

$$Q_a = \dot{m}C_{\mathrm{p},a}(T_o - T_i) = VI \tag{4}$$

The convective heat transfer from the test section can be expressed as

$$Q_{\mathrm{conv}} = hA\left(\tilde{T}_w - T_b\right) \tag{5}$$

in which

$$T_b = (\tilde{T}_o + T_i)/2 \tag{6}$$

$$\tilde{T}_o = \sum T_o/6 \tag{7}$$

and

$$\tilde{T}_w = \sum T_w/10 \tag{8}$$

T_w signifies the test tube's local wall temperature. Ten surface temperature measurements, evenly distributed between the tube's inlet and outlet, are used to calculate the average wall temperature. The mean Nusselt number (Nu) and the average heat transfer coefficient (h) are estimated using the following equations:

$$h = \dot{m}C_{\mathrm{p},a}(T_o - T_i)/A\left(\tilde{T}_w - T_b\right) \tag{9}$$

The Nusselt number (Nu) is used to evaluate heat transfer and can be calculated using the following equation:

$$\mathrm{Nu} = \frac{hD}{k} \tag{10}$$

All of thermo-physical properties of air are determined at the overall bulk air temperature (T_b) from Eq. (6). The thermal-performance enhancement factor (TEF), assessed at consistent pumping/blowing power [38-39] can be expressed as

$$\mathrm{TEF} = \left.\frac{h_b}{h_p}\right| = \left.\frac{Nu_b}{Nu_p}\right|_{pp} = \left(\frac{Nu_b}{Nu_p}\right)\left(\frac{f_b}{f_p}\right)^{-1/3} \tag{11}$$

where the heat transfer coefficients for the inserted tube and the plain tube are, respectively, h_b and h_p.

4. Results and Discussion

4.1 Plain tube verification

In the initial evaluation, the pressure loss and heat transfer, characterized by the friction factor (f) and Nusselt number (Nu), for the plain tube in the current study are compared and validated against standard correlations. Fig. 4 presents

a comparison between the experimental friction factor (f) and heat transfer (Nu) values from the plain tube and those predicted by the conventional Dittus-Boelter and Blasius correlations, as given in Eqs. (12) and (13).
The experimental data show good agreement with the correlation results, with an average deviation of around 6% for both Nu and f.

Dittus-Boelter correlation:

$$\mathrm{Nu} = 0.023\mathrm{Re}^{0.8}\mathrm{Pr}^{0.4} \tag{12}$$

Blasius correlation:

$$f = 0.316\ \mathrm{Re}^{-0.25} \tag{13}$$

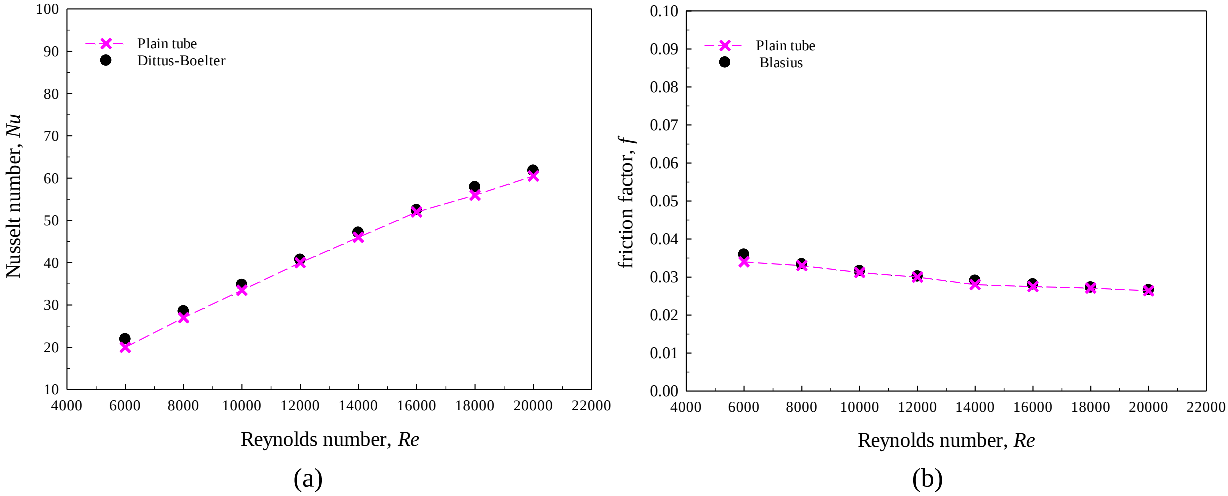

Fig. 4. Verification of Nu (a) and f (b) for correlation data compared to plain tube.

4.2. Heat transfer results

The effect of Delta winglet with various attack angles (θ)on Nu and Nu_b/Nu_p is illustrated in Fig. 5 (a) and (b), respectively. As shown in Fig. 5 (a), the insertion of the delta winglet (DW) significantly increases the Nusselt number compared to the plain tube in all scenarios. The delta winglet, strategically positioned at various attack angles, induces counter-rotating longitudinal vortices within the fluid flow. These vortices play a crucial role in enhancing convective heat transfer by disrupting the boundary layer that typically forms along the surface. This disruption increases fluid mixing near the wall, prolongs the residence time of the fluid, and improves the overall energy exchange between the heated surface and the cooler core fluid. At smaller attack angles, the sharper edges of the delta winglet intensify fluid impingement on the heat transfer surface, generating localized turbulence and increasing surface contact. This mechanism is particularly effective in promoting convective heat transfer, as the boundary layer is more effectively broken up, facilitating direct fluid interaction with the heated surface. Consequently, the implementation of the delta winglet leads to a substantial increase in the Nusselt number, ranging from 287% to 304% compared to a smooth tube. The highest heat transfer performance is achieved at an attack angle of 30°, where the vortices are optimally formed to maximize heat transfer. Additionally, the Nusselt number increases as the attack angle decreases. This is due to the narrower edges of the delta winglet (DW) at smaller attack angles, which create stronger fluid contact on the heat transfer surface, thereby further enhancing heat transfer performance.

Fig. 5 (b) illustrates the relationship between Nu_b/Nu_p and Re. The figure shows that as Re increases, the Nu ratio exhibits a slight fluctuation, with values rising between 2.51 and 3.04 times, influenced by θ and Re. Certainly, the highest Nu_b/Nu_p is observed for the DW at attack angle = 30°. The average Nu_b/Nu_p values of the DW at θ = 30°, 45° and 60° are around 3.04, 2.87; 2.85, 2.63 and 2.74, 2.51 times, respectively.

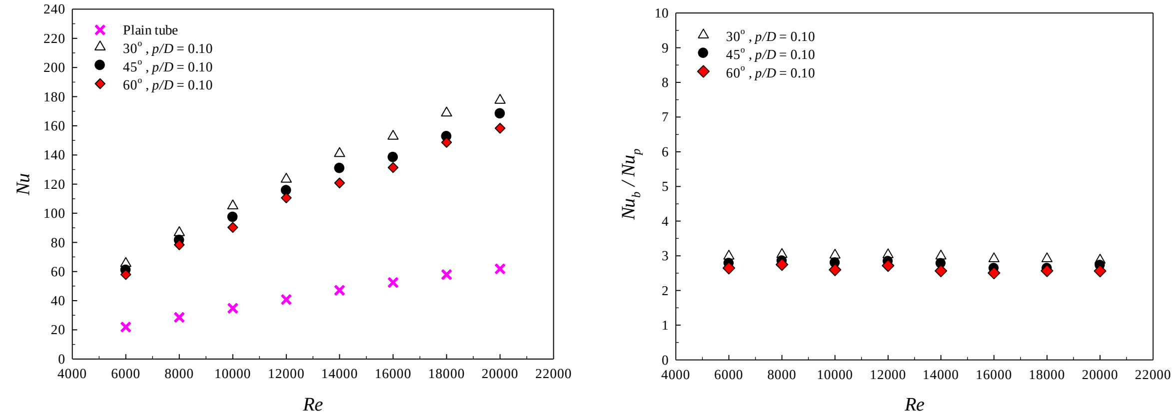

(a) Nu (b) Nu_b/Nu_p

Fig. 5. Variation of Nu and Nu_b/Nu_p with Re for Delta winglet insert

4.3. Friction factor results

Pressure loss or friction factor are presented as f and f_s/f_p by plotting against Re for the Delta winglet (DW) at different attack angle (θ) values, as illustrated in Fig. 6 (a) and (b). Fig. 6 (a) shows a pattern where the friction factor (f) decreases slightly as the Reynolds number (Re) increases. The installation of the delta winglet (DW) results in a significant increase in the friction factor compared to the smooth tube, indicating an increase in friction losses due to added flow obstruction. The scientific rationale behind this increase in friction loss is based on the effects of flow disturbances and pressure changes caused by the winglet's geometry. When the delta winglet is introduced into the flow, it obstructs the path, causing the fluid to navigate around it. This obstruction increases the contact area between the fluid and the surface, further intensifying drags forces. Additionally, the winglet generates counter-rotating vortices that disturb the flow, promoting turbulence. While this turbulence improves heat transfer, it also results in greater energy dissipation within the fluid, causing an increase in pressure drop along the channel. At lower attack angles (e.g., $\theta = 30°$), the winglet presents sharper edges to the incoming flow, which leads to more intense vortex generation and a higher degree of fluid mixing near the surface. This effect boosts both the heat transfer and the friction factor, as observed by the elevated friction factor ratios (f_s/f_p). Analysis of the figure reveals that the friction factor (f) increases as the attack angle (θ) decreases.

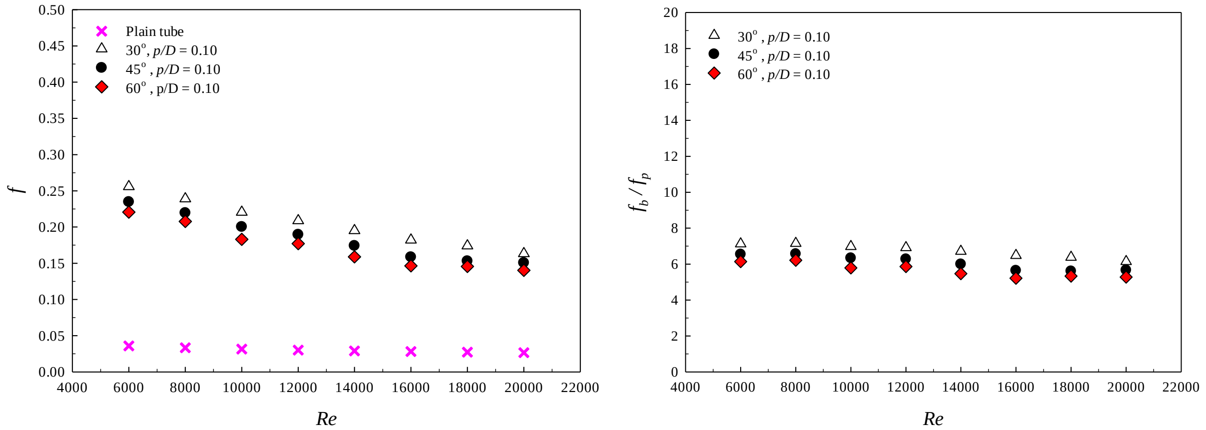

(a) f (b) f_s/f_p

Fig. 6. Variation of f and f_s/f_p with Re for Delta winglet insert

Fig. 6 (b) presents the relationship between the ratio of friction factors (f_s/f_p) and Reynolds number (Re) for the Delta winglet (DW) across various attack angles. The figure shows that as Re increases, the f_s/f_p ratio for the DW decreases slightly. The average f_s/f_p values for the tube with DW at $\theta = 30°$, 45° and 60° are approximately 6.74, 6.08 and 5.66, respectively. The highest f_s/f_p ratio of 7.15 is observed at an attack angle of $\theta = 30°$.

4.4 Thermal enhancement performance results

The variation of the thermal enhancement factor (TEF) with Reynolds number (*Re*) for the delta winglet (DW) at different attack angles (θ) is shown in Fig. 7. Notably, the TEF values are consistently above unity, indicating that the DW insert significantly improves the thermal-hydraulic performance compared to the smooth tube. For θ = 30°, the TEF slightly decreases as *Re* increases, while for θ = 45° and 60°, the TEF remains nearly unchanged. The maximum TEF of 1.34 is achieved at θ = 30° and *Re* = 6000, whereas the lowest TEF is found at θ = 60° and *Re* = 20,000. A closer analysis reveals that the DW with attack angles of 30°, 45° and 60° provides average TEF improvements of 31%, 23% and 13%, respectively, compared to the plain tube.

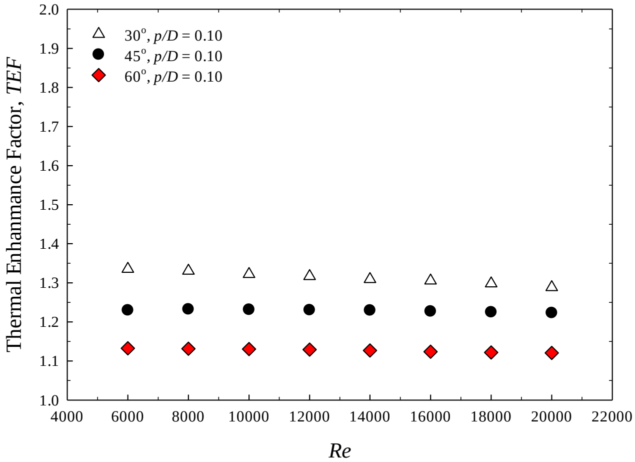

Fig. 7. Variation of TEF with *Re*

5. *Nu* and *f* correlations

The development of correlations has proven effective for predicting heat transfer, pressure loss, and the thermal enhancement factor (TEF), aiding in the design of heat exchangers and optimizing geometrical parameters for specific applications. Overall, the relationships between the Nusselt number (*Nu*) and TEF are strongly influenced by the geometrical and flow parameters, including the attack angle (θ), Reynolds number (*Re*), and Prandtl number (*Pr*), while the friction factor (*f*) remains unaffected by *Pr*. The empirical correlations for *Nu*, *f* and TEF, based on the experimental data for the delta winglet (DW), are presented as follows:

$$Nu = 0.133\, Re^{0.826}\, Pr^{0.4}\, \theta^{-0.234} \tag{14}$$

$$f = 24.231\, Re^{-0.393}\, \theta^{-0.318} \tag{15}$$

$$TEF = 3.683\, Re^{-0.014}\, \theta^{-0.262} \tag{16}$$

The predicted Nusselt number (*Nu*), friction factor (*f*), and thermal enhancement factor (TEF) for the DW inserts, as estimated by Eqs. (14) - (16), are compared with the experimental results in Fig. 8 (a), (b) and (c), respectively. The figure indicates that the experimental values for *Nu, f* and TEF deviate from the predicted values by ±4%, ±5% and ±3%, respectively. Thus, the developed correlations for *Nu*, *f* and TEF provide accurate predictions within the range of the studied DW parameters.

6. Statistical analysis

6.1 Main effect plot

The main effects plot visually represents the impact of each factor on the response variable, showing how changes in factor levels influence the outcome. It plots the mean response for each factor level, with a steeper slope indicating a stronger effect of that factor on the response signifying a significant impact on the outcome. In contrast, a flat line suggests that the factor has little to no effect, and varying its levels does not significantly alter the result. Main effects plots are particularly valuable for identifying trends and optimizing processes, as they allow for a clear comparison of factor levels and their influence on the response. The larger the change in the response variable across the levels of a factor, the more critical that factor is to the outcome.

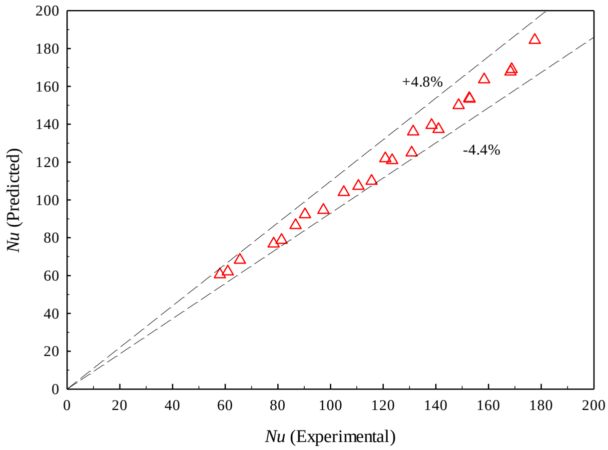

(a) *Nu*

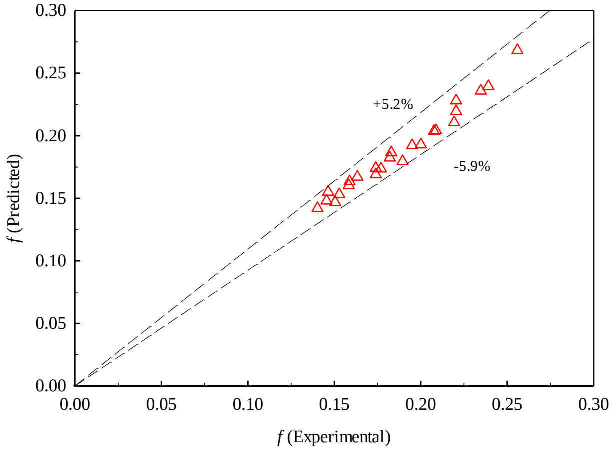

(b) *f*

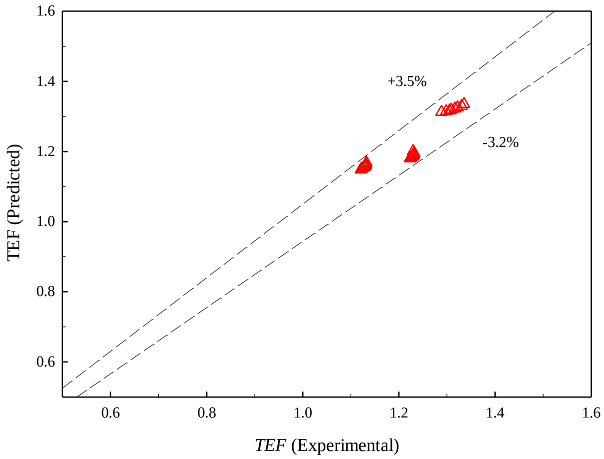

(c) TEF

Fig. 8. Predicted correlation and experimental data**:** (a) *Nu* , (b) *f* and (c) TEF

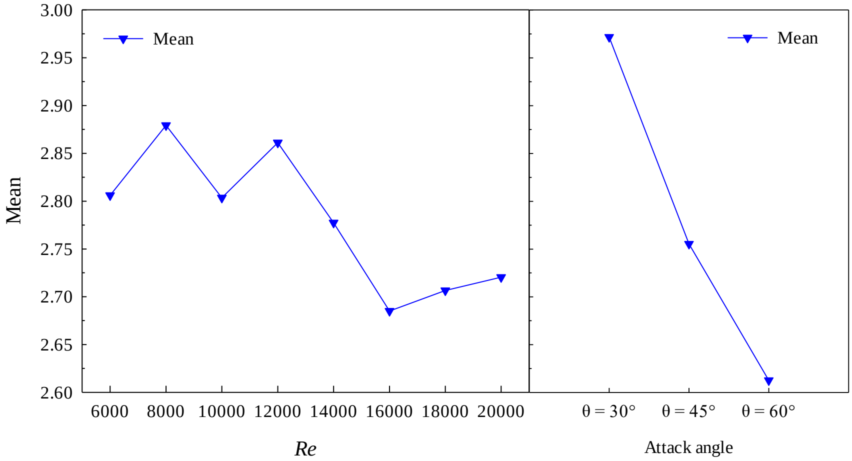

Fig. 9. Main effect of *Nu* ratio

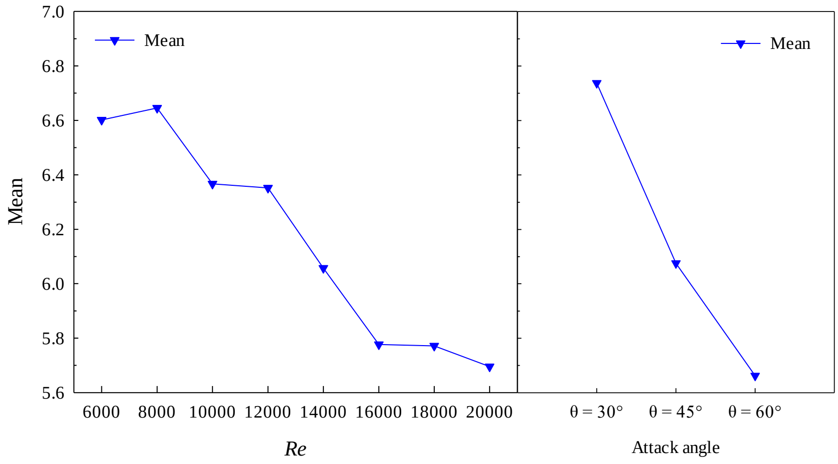

Fig. 10. Main effect of *f* ratio

Fig. 9. presents the main effects plot for the Nusselt number (*Nu*) ratio at Reynolds numbers (*Re*) ranging from 6000 to 20,000. The main effects plot *Nu* fluctuates and drops sharply below 2.7 at *Re* = 16,000. The effect of the attack angle at 30° is the highest (around 3.0), indicating the most significant enhancement in heat transfer. Fig. 10. shows the main effects plot for the friction factor (*f*) ratio with respect to *Re* and attack angle. The friction factor is above 6.2 at low *Re* values, gradually decreasing beyond *Re* of 12,000. Similar to that found for Nusselt number, the 30° attack angle produces a higher friction effect compared to the other angles.

6.2 Analysis of Variance (ANOVA)

ANOVA was implemented to conduct a statistical analysis of the findings. The robustness of the approach is predicted by ANOVA by determining specific statistical terms. In ANOVA, P-values less than 0.05 indicate that the model terms are "statistically significant," indicating that the corresponding factor has a substantial influence on the response. P values higher than 0.05 indicate that the model terms are "insignificant" and have been disregarded in subsequent analyses. Additionally, the regression model's considerable importance is demonstrated by its substantial F-value.

Factor information using *Re* = 6000, 8000, 10000, 12000, 14000, 16000, 18000, 20000 (levels=8), Attack angle(θ) levels =3 is 30°, 45° and 60°. The ANOVA table (Table 2) describes that *Re* has a significant impact on TEF, with a sum of squares (SS) of 0.001280 and a P-value of less than 0.05. Attack angle (θ) also contributes significantly to TEF variability, with a sum of squares (SS) of 0.139300 and a mean square of 0.069515. The error has 14 degrees of freedom, with a small SS of 0.000736, indicating that most of the variability is captured by *Re* and θ. The total sum of squares (SS) is 0.141045, indicating that *Re* and θ account for almost all the variance in *TEF*.

Table 2: ANOVA table for thermal enhancement factor

Factor	DF	Adj SS	Adj MS	F-Value	P-Value
Re	7	0.001280	0.000183	3.48	0.022
Attack angle(θ)	2	0.139030	0.069515	1322.78	0.000
Error	14	0.000736	0.000053		
Total	23	0.141045			

The model has an adjusted R-squared of 99.14%, indicating excellent fit to the data, with *Re* and θ explaining most variation in TEF. The predicted R-squared is 98.47%, confirming the model's ability to predict new data points outside the sample. The residual standard error is 0.0072493, confirming a good model fit. Table 3 illustrate the coefficients table shows the estimated regression coefficients for each level of Reynolds number (*Re*) and attack angle (θ). *Re* levels show significant effects on TEF, with coefficients 0.00958 at *Re* = 6000 and 0.00836 at *Re* = 8000. Other Re levels have non-significant coefficients. Attack angle (θ) has a strong positive effect at θ = 30° and a smaller positive effect at θ = 45°. The base level, θ = 60°, is not explicitly listed as the reference level in the regression model.

Fig. 11. illustrate the interaction plot of analysis reveals that Reynolds number and attack angle significantly impact the Thermal Enhancement Factor (*TEF*), with attack angle having a more significant impact especially $\theta = 30°$ at low *Re*.

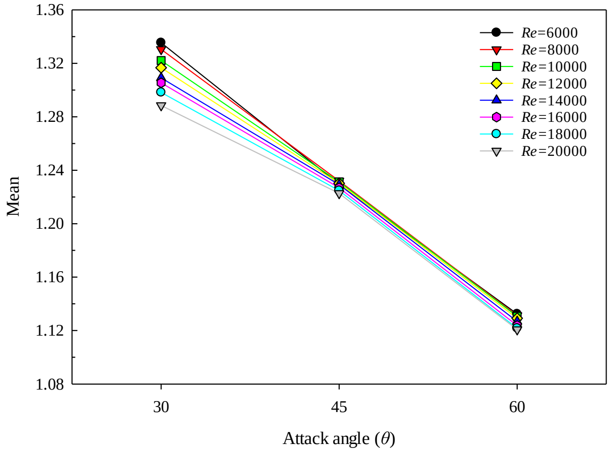

Fig. 11. Interaction of thermal enhancement factor

Table 3: Coefficients for thermal enhancement factor

	Term	Coef	SE Coef	T-Value	P-Value
Re					
	6000	0.00958	0.00392	2.45	0.028
	8000	0.00836	0.00392	2.14	0.051
	10000	0.00511	0.00392	1.31	0.213
	12000	0.00252	0.00392	0.64	0.531
	14000	-0.00116	0.00392	-0.30	0.772
	16000	-0.00421	0.00392	-1.08	0.300
	18000	-0.00795	0.00392	-2.03	0.062
Attack angle (θ)					
	θ =30°	0.09037	0.00209	43.18	0.000
	θ =45°	0.00545	0.00209	2.60	0.021

7. Conclusion

The study shows that incorporating Delta winglet (DW) inserts significantly enhances heat transfer within a copper tube. The creation of counter-rotating vortices by the DW inserts results in a 287-304% improvement in heat transfer compared to a plain tube. Additionally, the installation of DW inserts leads to a substantial increase in the friction factor compared to a smooth tube. Both heat transfer and friction loss rise as the attack angle decreases. The thermal enhancement factors (TEF) associated with the DW inserts consistently exceed unity, demonstrating a significant improvement in thermal-hydraulic performance over the smooth tube. The maximum TEF of 1.34 is achieved at an attack angle of 30° and a Reynolds number of 6000.

The empirical correlations for *Nu*, *f* and TEF demonstrated their effectiveness in forecasting the system's thermal and hydraulic performance, with discrepancies from experimental data remaining within acceptable limits. The ANOVA test confirmed that both the Reynolds number and the attack angle are important for figuring out how well thermal enhancement works, with the attack angle having a bigger effect when the Reynolds number is low. Overall, these findings highlight the potential of using Delta winglet (DW) inserts to improve the efficiency of heat exchangers in practical applications.

8. Acknowledgments

This research was financially supported and facilitated by the School of Engineering and Industrial Technology at Mahanakorn University of Technology.

Nomenclature

DW	Delta winglet
D	hydraulic diameter, mm
c	height of clearance, mm
f_p	friction factor
f_b	friction factor for a smooth channel
h	rib height, mm
h	convective heat transfer coefficient, W/m^2-K
I-VB	inclined V-shaped baffle
k	thermal conductivity of fluid, W/m-K
L	length of test section, mm
m_a	mass flow rate, kg/s
Nu_b	Nusselt number
Nu_p	Nusselt number for a smooth channel
P	pitch length, mm
PVC	Polyvinyl Chloride
Pr	Prandtl number
ΔP	pressure drop, Pa
Q	heat gained of air, W
Re	Reynolds number
T_b	bulk air temperature, K
T_i	inlet air temperature, K
T_o	outlet air temperature, K
TEF	thermal-performance enhancement factor
V	air velocity, m/s
θ	attack angle, degree
ρ	fluid density, kg/m^3
ν	kinematic viscosity, m^2/s

References

[1] Iqbal MH, Ahmed N, Ali M, Qaisrani MA, Mahmood M, Waqas A, Iqbal W, Sajid MB. Numerical analysis of a novel solar air heater design with V-ribs and jet cooling. Sustain Energy Technol Assess. 2023;57:103252.

[2] Singh VP, Jain S, Karn A, Dwivedi G, Kumar A, Mishra S, Sharma NK, Bajaj M, Zawbaa HM, Kamel S. Heat transfer and friction factor correlations development for double pass solar air heater artificially roughened with perforated multi-V ribs. Case Stud Therm Eng. 2022;39:102461.

[3] Krishnaswamy K, Sivan S. Improvement in thermal hydraulic performance by using continuous V and W-shaped rib turbulators in gas turbine blade cooling application. Case Stud Therm Eng. 2021;24:100857.

[4] Wang N, Ghoushchi SP, Sharma K, Elbadawy I, Mouldi A, Loukil H, Deifalla AF. Thermal performance enhancement in a double tube heat exchanger using combination of bubble injection and helical coiled wire insert. Case Stud Therm Eng. 2023;52:103722.

[5] García A, Vicente PG, Viedma A. Experimental study of heat transfer enhancement with wire coil inserts in laminar-transition-turbulent regimes at different Prandtl numbers. International J Heat Mass Transf. 2005;48(21–22):4640–4651.

[6] Gunes S, Ozceyhan V, Buyukalaca O. Heat transfer enhancement in a tube with equilateral triangle cross sectioned coiled wire inserts. Exp Therm Fluid Sci. 2010;34(6):684–691.

[7] Phila A, Keaitnukul W, Eiamsa-Ard S, Naphon P, Maruyama N, Hirota M, Chuwattanakul V. Influence of notched baffles on aerothermal performance behaviors in a channel. Case Stud Therm Eng. 2023;47:103070.

[8] Phila A, Eiamsa-Ard S, Thianpong C. Thermal performance evaluation of a channel installed with inclined-baffle turbulators. Arab J Sci Eng. 2019;45(2):609–621.

[9] Yuan M, Liu G, Zhang X, Zhang W, Yang Y, Song J, Lim H. Heat transfer enhancement for spiral finned tubes with triangular winglets. International J Heat Mass Transf. 2023;205:123918.

[10] Song K, Sun K, Lu X, Gao Q, Hou Q, Gu B. Effect of wavy delta winglet vortex generators on heat transfer performance of a fin-and-tube heat exchanger. International J Heat Fluid Flow. 2024;108:109485.

[11] Han H, Wang S, Sun L, Li Y, Wang S. Numerical study of thermal and flow characteristics for a fin-and-tube heat exchanger with arc winglet type vortex generators. International J Refrig. 2018;98:61–69.

[12] Biswas G, Mitra NK, Fiebig M. Heat transfer enhancement in fin-tube heat exchangers by winglet type vortex generators. International J Heat Mass Transf. 1994;37(2):283–291.

[13] Hoonpong P, Promthaisong P, Skullong S. Experimental study of thermal performance in a tubular heat exchanger using inclined perforated vortex rings. J Res Appl Mech Eng. 2020;8(2):148–157.

[14] Promthaisong P, Skullong S. Thermal characterization in circular tube inserted with diamond-shaped rings. J Res Appl Mech Eng. 2019;7(1):1–10.

[15] Göksu TT, Behçet R. Experimental investigation of the effect of a novel curved winglet vortex generator on heat transfer with a designed controller circuit. International J Therm Sci. 2022;180:107724.

[16] Lemenand T, Habchi C, Della Valle D, Peerhossaini H. Vorticity and convective heat transfer downstream of a vortex generator. International J Therm Sci. 2017;125:342–349.

[17] Wijayanta AT, Istanto T, Kariya K, Miyara A. Heat transfer enhancement of internal flow by inserting punched delta winglet vortex generators with various attack angles. Exp Therm Fluid Sci. 2017;87:141–148.

[18] Promvonge P, Jayranaiwachira N, Promthaisong P, Nakhchi E, Skullong S. Thermal effectiveness analysis of heat exchange tube with staggered louver-punched V-baffles. International Communications Heat Mass Transf. 2024;159:108052.

[19] Phila A, Chuwattanakul V, Thianpong C, Bhattacharyya S, Naphon P, Eiamsa-Ard S. Evaluation of aerothermal performance of a round tube with regularly-spaced multi-channel twisted tape elements installed. J Therm Anal Calorim. 2024;149(11):5543–5554.

[20] Eiamsa-Ard S, Thianpong C, Eiamsa-Ard P, Promvonge P. Convective heat transfer in a circular tube with short-length twisted tape insert. International Communications Heat Mass Transf. 2009;36(4):365–371.

[21] Nakhchi ME, Hatami M, Rahmati M. Experimental investigation of heat transfer enhancement of a heat exchanger tube equipped with double-cut twisted tapes. Appl Therm Eng. 2020;180:115863.

[22] Promvonge P, Skullong S. Augmented heat transfer in tubular heat exchanger fitted with V-baffled tapes. International J Therm Sci. 2020;155:106429.

[23] Suwannapan S, Skullong S, Promvonge P. Thermal characteristics in a heat exchanger tube fitted with zigzag-winglet perforated-tapes. J Res Appl Mech Eng. 2015;3:29–36.

[24] Promthaitsong P, Sumannapan S. Turbulent flow behaviors on thermal enhancement in a circular tube heat exchanger equipped with sinusoidal baffles. J Res Appl Mech Eng. 2018;6:95–112.

[25] Prasopsuk C, Hoonpong P, Skullong S, Promvonge P. Experimental investigation of thermal performance enhancement in tubular heat exchanger fitted with rectangular-winglet-tape vortex generator. Eng Appl Sci Res. 2016;43:279–282.

[26] Promthaitsong P, Sumannapan S. Thermal characterization in circular tube inserted with diamond-shaped rings. J Res Appl Mech Eng. 2019;7:1–10.

[27] Thianpong C, Yongsiri K, Nanan K, Eiamsa-Ard S. Thermal performance evaluation of heat exchangers fitted with twisted-ring turbulators. International Communications Heat Mass Transf. 2012;39(6):861–868.

[28] Singh V, Chamoli S, Kumar M, Kumar A. Heat transfer and fluid flow characteristics of heat exchanger tube with multiple twisted tapes and solid rings inserts. Chem Eng Process. 2016;102:156–168.

[29] Promvonge P, Skullong S. Augmented heat transfer in tubular heat exchanger fitted with V-baffled tapes. International J Therm Sci. 2020;155:106429.

[30] Rahman MA, Dhiman SK. Performance evaluation of turbulent circular heat exchanger with a novel flow deflector-type baffle plate. J Eng Res. 2023:100105.

[31] Jayranaiwachira N, Promvonge P, Thianpong C, Promthaisong P, Skullong S. Effect of louvered curved-baffles on thermohydraulic performance in heat exchanger tube. Case Stud Therm Eng. 2023;42:102717.

[32] Wang H, Abe AM, Al-Zubaidi A, Deifalla A, Galal AM, Zhou Y, Ghoushchi SP. Heat transfer enhancement of a copper tube with constant wall temperature using a novel horizontal perforated teardrop-shaped turbulators (PTST). International J Therm Sci. 2023;192:108418.

[33] Kumar A, Ali MA, Maithani R, Gupta NK, Sharma S, Kumar S, Sharma L, Thakur R, Alam T, Dobrota D, Eldin SM. Experimental analysis of heat exchanger using perforated conical rings, twisted tape inserts and CuO/H_2O nanofluids. Case Stud Therm Eng. 2023;49:103255.

[34] Ejaz F, Qasem NAA, Zubair SM. Thermal-hydraulic analysis of wetted airside plain fin flat tube heat exchangers and the role of vortex generators. Appl Therm Eng. 2024:124651.

[35] Song KW, Sun K, Lu X, Gao Q, Hou Q, Gu BD. Effect of wavy delta winglet vortex generators on heat transfer performance of a fin-and-tube heat exchanger. International J Heat Fluid Flow. 2024:109485.

[36] Yuan M, Liu G, Zhang X, Zhang W, Yang Y, Song J, Lim H. Heat transfer enhancement for spiral finned tubes with triangular winglets. International J Heat Mass Transf. 2023:123918.
[37] Heriyani O, Djaeni M, Syaiful, Putri AK. Perforated concave rectangular winglet pair vortex generators enhance the heat transfer of air flowing through heated tubes inside a channel. Results Eng. 2022:100705.
[38] Phila A, Thianpong C, Eiamsa-Ard S. Influence of geometric parameters of alternate axis twisted baffles on the local heat transfer distribution and pressure drop in a rectangular channel using a transient liquid crystal technique. Energies. 2019;12(12):2341.
[39] Promvonge P, Skullong S. Heat transfer in solar receiver heat exchanger with combined punched-V-ribs and chamfer-V-grooves. International J Heat Mass Transf. 2019;143:118486.